

Study of the $f_0(980)$ through the decay $D_s^+ \rightarrow \pi^+\pi^-e^+\nu_e$

- M. Ablikim¹, M. N. Achasov^{13,b}, P. Adlarson⁷⁵, R. Aliberti³⁶, A. Amoroso^{74A,74C}, M. R. An⁴⁰, Q. An^{71,58}, Y. Bai⁵⁷, O. Bakina³⁷, I. Balossino^{30A}, Y. Ban^{47,g}, V. Batozskaya^{1,45}, K. Begzsuren³³, N. Berger³⁶, M. Berlowski⁴⁵, M. Bertani^{29A}, D. Betttoni^{30A}, F. Bianchi^{74A,74C}, E. Bianco^{74A,74C}, J. Bloms⁶⁸, A. Bortone^{74A,74C}, I. Boyko³⁷, R. A. Briere⁵, A. Brueggemann⁶⁸, H. Cai⁷⁶, X. Cai^{1,58}, A. Calcaterra^{29A}, G. F. Cao^{1,63}, N. Cao^{1,63}, S. A. Cetin^{62A}, J. F. Chang^{1,58}, T. T. Chang⁷⁷, W. L. Chang^{1,63}, G. R. Che⁴⁴, G. Chelkov^{37,a}, C. Chen⁴⁴, Chao Chen⁵⁵, G. Chen¹, H. S. Chen^{1,63}, M. L. Chen^{1,58,63}, S. J. Chen⁴³, S. M. Chen⁶¹, T. Chen^{1,63}, X. R. Chen^{32,63}, X. T. Chen^{1,63}, Y. B. Chen^{1,58}, Y. Q. Chen³⁵, Z. J. Chen^{26,h}, W. S. Cheng^{74C}, S. K. Choi^{10A}, X. Chu⁴⁴, G. Cibinetto^{30A}, S. C. Coen⁴, F. Cossio^{74C}, J. J. Cui⁵⁰, H. L. Dai^{1,58}, J. P. Dai⁷⁹, A. Dbeysi¹⁹, R. E. de Boer⁴, D. Dedovich³⁷, Z. Y. Deng¹, A. Denig³⁶, I. Denysenko³⁷, M. Destefanis^{74A,74C}, F. De Mori^{74A,74C}, B. Ding^{66,1}, X. X. Ding^{47,g}, Y. Ding³⁵, Y. Ding⁴¹, J. Dong^{1,58}, L. Y. Dong^{1,63}, M. Y. Dong^{1,58,63}, X. Dong⁷⁶, S. X. Du⁸¹, Z. H. Duan⁴³, P. Egorov^{37,a}, Y. L. Fan⁷⁶, J. Fang^{1,58}, S. S. Fang^{1,63}, W. X. Fang¹, Y. Fang¹, R. Farinelli^{30A}, L. Fava^{74B,74C}, F. Feldbauer⁴, G. Felici^{29A}, C. Q. Feng^{71,58}, J. H. Feng⁵⁹, K. Fischer⁶⁹, M. Fritsch⁴, C. Fritzsch⁶⁸, C. D. Fu¹, J. L. Fu⁶³, Y. W. Fu¹, H. Gao⁶³, Y. N. Gao^{47,g}, Yang Gao^{71,58}, S. Garbolino^{74C}, I. Garzia^{30A,30B}, P. T. Ge⁷⁶, Z. W. Ge⁴³, C. Geng⁵⁹, E. M. Gersabeck⁶⁷, A. Gilman⁶⁹, K. Goetzen¹⁴, L. Gong⁴¹, W. X. Gong^{1,58}, W. Gradl³⁶, S. Gramigna^{30A,30B}, M. Greco^{74A,74C}, M. H. Gu^{1,58}, Y. T. Gu¹⁶, C. Y. Guan^{1,63}, Z. L. Guan²³, A. Q. Guo^{32,63}, L. B. Guo⁴², R. P. Guo⁴⁹, Y. P. Guo^{12,f}, A. Guskov^{37,a}, X. T. H.^{1,63}, T. T. Han⁵⁰, W. Y. Han⁴⁰, X. Q. Hao²⁰, F. A. Harris⁶⁵, K. K. He⁵⁵, K. L. He^{1,63}, F. H. H.. Heinsius⁴, C. H. Heinz³⁶, Y. K. Heng^{1,58,63}, C. Herold⁶⁰, T. Holtmann⁴, P. C. Hong^{12,f}, G. Y. Hou^{1,63}, Y. R. Hou⁶³, Z. L. Hou¹, H. M. Hu^{1,63}, J. F. Hu^{56,i}, T. Hu^{1,58,63}, Y. Hu¹, G. S. Huang^{71,58}, K. X. Huang⁵⁹, L. Q. Huang^{32,63}, X. T. Huang⁵⁰, Y. P. Huang¹, T. Hussain⁷³, N Hüsken^{28,36}, W. Imoehl²⁸, M. Irshad^{71,58}, J. Jackson²⁸, S. Jaeger⁴, S. Janchiv³³, J. H. Jeong^{10A}, Q. Ji¹, Q. P. Ji²⁰, X. B. Ji^{1,63}, X. L. Ji^{1,58}, Y. Y. Ji⁵⁰, Z. K. Jia^{71,58}, P. C. Jiang^{47,g}, S. S. Jiang⁴⁰, T. J. Jiang¹⁷, X. S. Jiang^{1,58,63}, Y. Jiang⁶³, J. B. Jiao⁵⁰, Z. Jiao²⁴, S. Jin⁴³, Y. Jin⁶⁶, M. Q. Jing^{1,63}, T. Johansson⁷⁵, X. K.¹, S. Kabana³⁴, N. Kalantar-Nayestanaki⁶⁴, X. L. Kang⁹, X. S. Kang⁴¹, R. Kappert⁶⁴, M. Kavatsyuk⁶⁴, B. C. Ke⁸¹, A. Khoukaz⁶⁸, R. Kiuchi¹, R. Kliemt¹⁴, L. Koch³⁸, O. B. Kolcu^{62A}, B. Kopf⁴, M. K. Kuessner⁴, A. Kupsc^{45,75}, W. Kühn³⁸, J. J. Lane⁶⁷, J. S. Lange³⁸, P. Larin¹⁹, A. Lavania²⁷, L. Lavezzi^{74A,74C}, T. T. Lei^{71,k}, Z. H. Lei^{71,58}, H. Leithoff³⁶, M. Lellmann³⁶, T. Lenz³⁶, C. Li⁴⁸, C. Li⁴⁴, C. H. Li⁴⁰, Cheng Li^{71,58}, D. M. Li⁸¹, F. Li^{1,58}, G. Li¹, H. Li^{71,58}, H. B. Li^{1,63}, H. J. Li²⁰, H. N. Li^{56,i}, Hui Li⁴⁴, J. R. Li⁶¹, J. S. Li⁵⁹, J. W. Li⁵⁰, Ke Li¹, L. J. Li^{1,63}, L. K. Li¹, Lei Li³, M. H. Li⁴⁴, P. R. Li^{39,j,k}, S. X. Li¹², T. Li⁵⁰, W. D. Li^{1,63}, W. G. Li¹, X. H. Li^{71,58}, X. L. Li⁵⁰, Xiaoyu Li^{1,63}, Y. G. Li^{47,g}, Z. J. Li⁵⁹, Z. X. Li¹⁶, Z. Y. Li⁵⁹, C. Liang⁴³, H. Liang^{71,58}, H. Liang³⁵, H. Liang^{1,63}, Y. F. Liang⁵⁴, Y. T. Liang^{32,63}, G. R. Liao¹⁵, L. Z. Liao⁵⁰, J. Libby²⁷, A. Limphirat⁶⁰, D. X. Lin^{32,63}, T. Lin¹, B. J. Liu¹, B. X. Liu⁷⁶, C. Liu³⁵, C. X. Liu¹, D. Liu^{19,71}, F. H. Liu⁵³, Fang Liu¹, Feng Liu⁶, G. M. Liu^{56,i}, H. Liu^{39,j,k}, H. B. Liu¹⁶, H. M. Liu^{1,63}, Huanhuan Liu¹, Huihui Liu²², J. B. Liu^{71,58}, J. L. Liu⁷², J. Y. Liu^{1,63}, K. Liu¹, K. Y. Liu⁴¹, Ke Liu²³, L. Liu^{71,58}, L. C. Liu⁴⁴, Lu Liu⁴⁴, M. H. Liu^{12,f}, P. L. Liu¹, Q. Liu⁶³, S. B. Liu^{71,58}, T. Liu^{12,f}, W. K. Liu⁴⁴, W. M. Liu^{71,58}, X. Liu^{39,j,k}, Y. Liu^{39,j,k}, Y. B. Liu⁴⁴, Z. A. Liu^{1,58,63}, Z. Q. Liu⁵⁰, X. C. Lou^{1,58,63}, F. X. Lu⁵⁹, H. J. Lu²⁴, J. G. Lu^{1,58}, X. L. Lu¹, Y. Lu⁷, Y. P. Lu^{1,58}, Z. H. Lu^{1,63}, C. L. Luo⁴², M. X. Luo⁸⁰, T. Luo^{12,f}, X. L. Luo^{1,58}, X. R. Lyu⁶³, Y. F. Lyu⁴⁴, F. C. Ma⁴¹, H. L. Ma¹, J. L. Ma^{1,63}, L. L. Ma⁵⁰, M. M. Ma^{1,63}, Q. M. Ma¹, R. Q. Ma^{1,63}, R. T. Ma⁶³, X. Y. Ma^{1,58}, Y. Ma^{47,g}, Y. M. Ma³², F. E. Maas¹⁹, M. Maggiora^{74A,74C}, S. Maldaner⁴, S. Malde⁶⁹, A. Mangoni^{29B}, Y. J. Mao^{47,g}, Z. P. Mao¹, S. Marcello^{74A,74C}, Z. X. Meng⁶⁶, J. G. Messchendorp^{14,64}, G. Mezzadri^{30A}, H. Miao^{1,63}, T. J. Min⁴³, R. E. Mitchell²⁸, X. H. Mo^{1,58,63}, N. Yu. Muchnoi^{13,b}, Y. Nefedov³⁷, F. Nerling^{19,d}, I. B. Nikolaev^{13,b}, Z. Ning^{1,58}, S. Nisar^{11,l}, Y. Niu⁵⁰, S. L. Olsen⁶³, Q. Ouyang^{1,58,63}, S. Pacetti^{29B,29C}, X. Pan⁵⁵, Y. Pan⁵⁷, A. Pathak³⁵, P. Patteri^{29A}, Y. P. Pei^{71,58}, M. Pelizaeus⁴, H. P. Peng^{71,58}, K. Peters^{14,d}, J. L. Ping⁴², R. G. Ping^{1,63}, S. Plura³⁶, S. Pogodin³⁷, V. Prasad³⁴, F. Z. Qi¹, H. Qi^{71,58}, H. R. Qi⁶¹, M. Qi⁴³, T. Y. Qi^{12,f}, S. Qian^{1,58}, W. B. Qian⁶³, C. F. Qiao⁶³, J. J. Qin⁷², L. Q. Qin¹⁵, X. P. Qin^{12,f}, X. S. Qin⁵⁰, Z. H. Qin^{1,58}, J. F. Qiu¹, S. Q. Qu⁶¹, C. F. Redmer³⁶, K. J. Ren⁴⁰, A. Rivetti^{74C}, V. Rodin⁶⁴, M. Rolo^{74C}, G. Rong^{1,63}, Ch. Rosner¹⁹, S. N. Ruan⁴⁴, N. Salone⁴⁵, A. Sarantsev^{37,c}, Y. Schelhaas³⁶, K. Schoenning⁷⁵, M. Scodeggio^{30A,30B}, K. Y. Shan^{12,f}, W. Shan²⁵, X. Y. Shan^{71,58}, J. F. Shangguan⁵⁵, L. G. Shao^{1,63}, M. Shao^{71,58}, C. P. Shen^{12,f}, H. F. Shen^{1,63}, W. H. Shen⁶³, X. Y. Shen^{1,63}, B. A. Shi⁶³, H. C. Shi^{71,58}, J. L. Shi¹², J. Y. Shi¹, Q. Q. Shi⁵⁵, R. S. Shi^{1,63}, X. Shi^{1,58}, J. J. Song²⁰, T. Z. Song⁵⁹, W. M. Song^{35,1}, Y. J. Song¹², Y. X. Song^{47,g}, S. Sosio^{74A,74C}, S. Spataro^{74A,74C}, F. Stieler³⁶, Y. J. Su⁶³, G. B. Sun⁷⁶, G. X. Sun¹, H. Sun⁶³, H. K. Sun¹, J. F. Sun²⁰, K. Sun⁶¹, L. Sun⁷⁶, S. S. Sun^{1,63},

T. Sun^{1,63}, W. Y. Sun³⁵, Y. Sun⁹, Y. J. Sun^{71,58}, Y. Z. Sun¹, Z. T. Sun⁵⁰, Y. X. Tan^{71,58}, C. J. Tang⁵⁴, G. Y. Tang¹, J. Tang⁵⁹, Y. A. Tang⁷⁶, L. Y. Tao⁷², Q. T. Tao^{26,h}, M. Tat⁶⁹, J. X. Teng^{71,58}, V. Thoren⁷⁵, W. H. Tian⁵⁹, W. H. Tian⁵², Y. Tian^{32,63}, Z. F. Tian⁷⁶, I. Uman^{62B}, B. Wang¹, B. L. Wang⁶³, Bo Wang^{71,58}, C. W. Wang⁴³, D. Y. Wang^{47,g}, F. Wang⁷², H. J. Wang^{39,j,k}, H. P. Wang^{1,63}, K. Wang^{1,58}, L. L. Wang¹, M. Wang⁵⁰, Meng Wang^{1,63}, S. Wang^{12,f}, S. Wang^{39,j,k}, T. Wang^{12,f}, T. J. Wang⁴⁴, W. Wang⁵⁹, W. Wang⁷², W. H. Wang⁷⁶, W. P. Wang^{71,58}, X. Wang^{47,g}, X. F. Wang^{39,j,k}, X. J. Wang⁴⁰, X. L. Wang^{12,f}, Y. Wang⁶¹, Y. D. Wang⁴⁶, Y. F. Wang^{1,58,63}, Y. H. Wang⁴⁸, Y. N. Wang⁴⁶, Y. Q. Wang¹, Yaqian Wang^{18,1}, Yi Wang⁶¹, Z. Wang^{1,58}, Z. L. Wang⁷², Z. Y. Wang^{1,63}, Ziyi Wang⁶³, D. Wei⁷⁰, D. H. Wei¹⁵, F. Weidner⁶⁸, S. P. Wen¹, C. W. Wenzel⁴, U. W. Wiedner⁴, G. Wilkinson⁶⁹, M. Wolke⁷⁵, L. Wollenberg⁴, C. Wu⁴⁰, J. F. Wu^{1,63}, L. H. Wu¹, L. J. Wu^{1,63}, X. Wu^{12,f}, X. H. Wu³⁵, Y. Wu⁷¹, Y. J. Wu³², Z. Wu^{1,58}, L. Xia^{71,58}, X. M. Xian⁴⁰, T. Xiang^{47,g}, D. Xiao^{39,j,k}, G. Y. Xiao⁴³, H. Xiao^{12,f}, S. Y. Xiao¹, Y. L. Xiao^{12,f}, Z. J. Xiao⁴², C. Xie⁴³, X. H. Xie^{47,g}, Y. Xie⁵⁰, Y. G. Xie^{1,58}, Y. H. Xie⁶, Z. P. Xie^{71,58}, T. Y. Xing^{1,63}, C. F. Xu^{1,63}, C. J. Xu⁵⁹, G. F. Xu¹, H. Y. Xu⁶⁶, Q. J. Xu¹⁷, Q. N. Xu³¹, W. Xu^{1,63}, W. L. Xu⁶⁶, X. P. Xu⁵⁵, Y. C. Xu⁷⁸, Z. P. Xu⁴³, Z. S. Xu⁶³, F. Yan^{12,f}, L. Yan^{12,f}, W. B. Yan^{71,58}, W. C. Yan⁸¹, X. Q. Yan¹, H. J. Yang^{51,e}, H. L. Yang³⁵, H. X. Yang¹, Tao Yang¹, Y. Yang^{12,f}, Y. F. Yang⁴⁴, Y. X. Yang^{1,63}, Yifan Yang^{1,63}, Z. W. Yang^{39,j,k}, M. Ye^{1,58}, M. H. Ye⁸, J. H. Yin¹, Z. Y. You⁵⁹, B. X. Yu^{1,58,63}, C. X. Yu⁴⁴, G. Yu^{1,63}, J. S. Yu^{26,h}, T. Yu⁷², X. D. Yu^{47,g}, C. Z. Yuan^{1,63}, L. Yuan², S. C. Yuan¹, X. Q. Yuan¹, Y. Yuan^{1,63}, Z. Y. Yuan⁵⁹, C. X. Yue⁴⁰, A. A. Zafar⁷³, F. R. Zeng⁵⁰, X. Zeng^{12,f}, Y. Zeng^{26,h}, Y. J. Zeng^{1,63}, X. Y. Zhai³⁵, Y. H. Zhan⁵⁹, A. Q. Zhang^{1,63}, B. L. Zhang^{1,63}, B. X. Zhang¹, D. H. Zhang⁴⁴, G. Y. Zhang²⁰, H. Zhang⁷¹, H. H. Zhang⁵⁹, H. H. Zhang³⁵, H. Q. Zhang^{1,58,63}, H. Y. Zhang^{1,58}, J. J. Zhang⁵², J. L. Zhang²¹, J. Q. Zhang⁴², J. W. Zhang^{1,58,63}, J. X. Zhang^{39,j,k}, J. Y. Zhang¹, J. Z. Zhang^{1,63}, Jianyu Zhang⁶³, Jiawei Zhang^{1,63}, L. M. Zhang⁶¹, L. Q. Zhang⁵⁹, Lei Zhang⁴³, P. Zhang¹, Q. Y. Zhang^{40,81}, Shuihan Zhang^{1,63}, Shulei Zhang^{26,h}, X. D. Zhang⁴⁶, X. M. Zhang¹, X. Y. Zhang⁵⁰, X. Y. Zhang⁵⁵, Y. Zhang⁶⁹, Y. Zhang⁷², Y. T. Zhang⁸¹, Y. H. Zhang^{1,58}, Yan Zhang^{71,58}, Yao Zhang¹, Z. H. Zhang¹, Z. L. Zhang³⁵, Z. Y. Zhang⁴⁴, Z. Y. Zhang⁷⁶, G. Zhao¹, J. Zhao⁴⁰, J. Y. Zhao^{1,63}, J. Z. Zhao^{1,58}, Lei Zhao^{71,58}, Ling Zhao¹, M. G. Zhao⁴⁴, S. J. Zhao⁸¹, Y. B. Zhao^{1,58}, Y. X. Zhao^{32,63}, Z. G. Zhao^{71,58}, A. Zhemchugov^{37,a}, B. Zheng⁷², J. P. Zheng^{1,58}, W. J. Zheng^{1,63}, Y. H. Zheng⁶³, B. Zhong⁴², X. Zhong⁵⁹, H. Zhou⁵⁰, L. P. Zhou^{1,63}, X. Zhou⁷⁶, X. K. Zhou⁶, X. R. Zhou^{71,58}, X. Y. Zhou⁴⁰, Y. Z. Zhou^{12,f}, J. Zhu⁴⁴, K. Zhu¹, K. J. Zhu^{1,58,63}, L. Zhu³⁵, L. X. Zhu⁶³, S. H. Zhu⁷⁰, S. Q. Zhu⁴³, T. J. Zhu^{12,f}, W. J. Zhu^{12,f}, Y. C. Zhu^{71,58}, Z. A. Zhu^{1,63}, J. H. Zou¹, J. Zu^{71,58}

(BESIII Collaboration)

¹ Institute of High Energy Physics, Beijing 100049, People's Republic of China

² Beihang University, Beijing 100191, People's Republic of China

³ Beijing Institute of Petrochemical Technology, Beijing 102617, People's Republic of China

⁴ Bochum Ruhr-University, D-44780 Bochum, Germany

⁵ Carnegie Mellon University, Pittsburgh, Pennsylvania 15213, USA

⁶ Central China Normal University, Wuhan 430079, People's Republic of China

⁷ Central South University, Changsha 410083, People's Republic of China

⁸ China Center of Advanced Science and Technology, Beijing 100190, People's Republic of China

⁹ China University of Geosciences, Wuhan 430074, People's Republic of China

¹⁰ Chung-Ang University, Seoul, 06974, Republic of Korea

¹¹ COMSATS University Islamabad, Lahore Campus, Defence Road, Off Raiwind Road, 54000 Lahore, Pakistan

¹² Fudan University, Shanghai 200433, People's Republic of China

¹³ G.I. Budker Institute of Nuclear Physics SB RAS (BINP), Novosibirsk 630090, Russia

¹⁴ GSI Helmholtzcentre for Heavy Ion Research GmbH, D-64291 Darmstadt, Germany

¹⁵ Guangxi Normal University, Guilin 541004, People's Republic of China

¹⁶ Guangxi University, Nanning 530004, People's Republic of China

¹⁷ Hangzhou Normal University, Hangzhou 310036, People's Republic of China

¹⁸ Hebei University, Baoding 071002, People's Republic of China

¹⁹ Helmholtz Institute Mainz, Staudinger Weg 18, D-55099 Mainz, Germany

²⁰ Henan Normal University, Xinxiang 453007, People's Republic of China

²¹ Henan University, Kaifeng 475004, People's Republic of China

²² Henan University of Science and Technology, Luoyang 471003, People's Republic of China

- ²³ Henan University of Technology, Zhengzhou 450001, People's Republic of China
²⁴ Huangshan College, Huangshan 245000, People's Republic of China
²⁵ Hunan Normal University, Changsha 410081, People's Republic of China
²⁶ Hunan University, Changsha 410082, People's Republic of China
²⁷ Indian Institute of Technology Madras, Chennai 600036, India
²⁸ Indiana University, Bloomington, Indiana 47405, USA
- ²⁹ INFN Laboratori Nazionali di Frascati , (A)INFN Laboratori Nazionali di Frascati, I-00044, Frascati, Italy; (B)INFN Sezione di Perugia, I-06100, Perugia, Italy; (C)University of Perugia, I-06100, Perugia, Italy
³⁰ INFN Sezione di Ferrara, (A)INFN Sezione di Ferrara, I-44122, Ferrara, Italy; (B)University of Ferrara, I-44122, Ferrara, Italy
- ³¹ Inner Mongolia University, Hohhot 010021, People's Republic of China
³² Institute of Modern Physics, Lanzhou 730000, People's Republic of China
³³ Institute of Physics and Technology, Peace Avenue 54B, Ulaanbaatar 13330, Mongolia
³⁴ Instituto de Alta Investigación, Universidad de Tarapacá, Casilla 7D, Arica, Chile
³⁵ Jilin University, Changchun 130012, People's Republic of China
- ³⁶ Johannes Gutenberg University of Mainz, Johann-Joachim-Becher-Weg 45, D-55099 Mainz, Germany
³⁷ Joint Institute for Nuclear Research, 141980 Dubna, Moscow region, Russia
- ³⁸ Justus-Liebig-Universitaet Giessen, II. Physikalisches Institut, Heinrich-Buff-Ring 16, D-35392 Giessen, Germany
³⁹ Lanzhou University, Lanzhou 730000, People's Republic of China
⁴⁰ Liaoning Normal University, Dalian 116029, People's Republic of China
⁴¹ Liaoning University, Shenyang 110036, People's Republic of China
⁴² Nanjing Normal University, Nanjing 210023, People's Republic of China
⁴³ Nanjing University, Nanjing 210093, People's Republic of China
⁴⁴ Nankai University, Tianjin 300071, People's Republic of China
⁴⁵ National Centre for Nuclear Research, Warsaw 02-093, Poland
- ⁴⁶ North China Electric Power University, Beijing 102206, People's Republic of China
⁴⁷ Peking University, Beijing 100871, People's Republic of China
⁴⁸ Qufu Normal University, Qufu 273165, People's Republic of China
⁴⁹ Shandong Normal University, Jinan 250014, People's Republic of China
⁵⁰ Shandong University, Jinan 250100, People's Republic of China
- ⁵¹ Shanghai Jiao Tong University, Shanghai 200240, People's Republic of China
⁵² Shanxi Normal University, Linfen 041004, People's Republic of China
⁵³ Shanxi University, Taiyuan 030006, People's Republic of China
⁵⁴ Sichuan University, Chengdu 610064, People's Republic of China
⁵⁵ Soochow University, Suzhou 215006, People's Republic of China
- ⁵⁶ South China Normal University, Guangzhou 510006, People's Republic of China
⁵⁷ Southeast University, Nanjing 211100, People's Republic of China
⁵⁸ State Key Laboratory of Particle Detection and Electronics, Beijing 100049, Hefei 230026, People's Republic of China
- ⁵⁹ Sun Yat-Sen University, Guangzhou 510275, People's Republic of China
- ⁶⁰ Suranaree University of Technology, University Avenue 111, Nakhon Ratchasima 30000, Thailand
⁶¹ Tsinghua University, Beijing 100084, People's Republic of China
- ⁶² Turkish Accelerator Center Particle Factory Group, (A)Istinye University, 34010, Istanbul, Turkey; (B)Near East University, Nicosia, North Cyprus, 99138, Mersin 10, Turkey
- ⁶³ University of Chinese Academy of Sciences, Beijing 100049, People's Republic of China
⁶⁴ University of Groningen, NL-9747 AA Groningen, The Netherlands
⁶⁵ University of Hawaii, Honolulu, Hawaii 96822, USA
⁶⁶ University of Jinan, Jinan 250022, People's Republic of China
- ⁶⁷ University of Manchester, Oxford Road, Manchester, M13 9PL, United Kingdom
⁶⁸ University of Muenster, Wilhelm-Klemm-Strasse 9, 48149 Muenster, Germany
⁶⁹ University of Oxford, Keble Road, Oxford OX13RH, United Kingdom

⁷⁰ University of Science and Technology Liaoning, Anshan 114051, People's Republic of China

⁷¹ University of Science and Technology of China, Hefei 230026, People's Republic of China

⁷² University of South China, Hengyang 421001, People's Republic of China

⁷³ University of the Punjab, Lahore-54590, Pakistan

⁷⁴ University of Turin and INFN, (A)University of Turin, I-10125, Turin, Italy; (B)University of Eastern Piedmont, I-15121, Alessandria, Italy; (C)INFN, I-10125, Turin, Italy

⁷⁵ Uppsala University, Box 516, SE-75120 Uppsala, Sweden

⁷⁶ Wuhan University, Wuhan 430072, People's Republic of China

⁷⁷ Xinyang Normal University, Xinyang 464000, People's Republic of China

⁷⁸ Yantai University, Yantai 264005, People's Republic of China

⁷⁹ Yunnan University, Kunming 650500, People's Republic of China

⁸⁰ Zhejiang University, Hangzhou 310027, People's Republic of China

⁸¹ Zhengzhou University, Zhengzhou 450001, People's Republic of China

^a Also at the Moscow Institute of Physics and Technology, Moscow 141700, Russia

^b Also at the Novosibirsk State University, Novosibirsk, 630090, Russia

^c Also at the NRC "Kurchatov Institute", PNPI, 188300, Gatchina, Russia

^d Also at Goethe University Frankfurt, 60323 Frankfurt am Main, Germany

^e Also at Key Laboratory for Particle Physics, Astrophysics and Cosmology, Ministry of Education; Shanghai Key Laboratory for Particle Physics and Cosmology; Institute of Nuclear and Particle Physics, Shanghai 200240, People's Republic of China

^f Also at Key Laboratory of Nuclear Physics and Ion-beam Application (MOE) and Institute of Modern Physics, Fudan University, Shanghai 200443, People's Republic of China

^g Also at State Key Laboratory of Nuclear Physics and Technology, Peking University, Beijing 100871, People's Republic of China

^h Also at School of Physics and Electronics, Hunan University, Changsha 410082, China

ⁱ Also at Guangdong Provincial Key Laboratory of Nuclear Science, Institute of Quantum Matter, South China Normal University, Guangzhou 510006, China

^j Also at Frontiers Science Center for Rare Isotopes, Lanzhou University, Lanzhou 730000, People's Republic of China

^k Also at Lanzhou Center for Theoretical Physics, Lanzhou University, Lanzhou 730000, People's Republic of China

^l Also at the Department of Mathematical Sciences, IBA, Karachi 75270, Pakistan

(Dated: March 24, 2023)

Using e^+e^- collision data corresponding to an integrated luminosity of 7.33 fb^{-1} recorded by the BESIII detector at center-of-mass energies between 4.128 and 4.226 GeV, we present an analysis of the decay $D_s^+ \rightarrow f_0(980)e^+\nu_e$ with $f_0(980) \rightarrow \pi^+\pi^-$, where the D_s^+ is produced via the process $e^+e^- \rightarrow D_s^{*\pm}D_s^{\mp}$. We observe the $f_0(980)$ in the $\pi^+\pi^-$ system and the branching fraction of the decay $D_s^+ \rightarrow f_0(980)e^+\nu_e$ with $f_0(980) \rightarrow \pi^+\pi^-$ is measured to be $(1.72 \pm 0.13_{\text{stat}} \pm 0.10_{\text{syst}}) \times 10^{-3}$, where the uncertainties are statistical and systematic, respectively. The dynamics of the $D_s^+ \rightarrow f_0(980)e^+\nu_e$ decay are studied with the simple pole parameterization of the hadronic form factor and the Flatté formula describing the $f_0(980)$ in the differential decay rate, and the product of the form factor $f_+^{f_0}(0)$ and the $c \rightarrow s$ Cabibbo-Kobayashi-Maskawa matrix element $|V_{cs}|$ is determined for the first time to be $f_+^{f_0}(0)|V_{cs}| = 0.504 \pm 0.017_{\text{stat}} \pm 0.035_{\text{syst}}$.

Quantum Chromodynamics (QCD), the fundamental theory of the Strong Interaction, has been established for almost half a century. However, there are some features that still need to be understood, such as quark confinement and dynamics in the non-perturbative regime. The light scalar mesons $f_0(500)$, $f_0(980)$, and $a_0(980)$ play a crucial role in the dynamics of the spontaneous breaking of QCD chiral symmetry and in the origin of pseudoscalar meson masses [1, 2], and consequently can be used to probe the confinement of quarks [3]. Furthermore, our understanding of the nature of light hadrons is still poor

since QCD is non-perturbative in the low-energy region. Investigating the structure of the light scalar mesons provides key input to these issues. In spite of the striking success of the constituent quark model, the nontrivial quark structure of these mesons has remained controversial for many years [4]. Their mass ordering cannot be explained by a $q\bar{q}$ configuration in the naive quark model, leaving open the possibility that they are mixtures of $q\bar{q}$ states [3, 5–12]. Other interpretations are diquark-antidiquark states (tetraquark) [13] and meson-meson bound states (molecule) [14]. Therefore, more conclu-

sive experimental measurements of these scalar states are highly desired.

Since the leptons and hadrons in the final state interact only weakly with each other, the semileptonic (SL) decays of charm mesons provide a unique and clean platform to probe the constituent $q\bar{q}$ components in the wave functions of light scalar states [15]. Here, only the spectator light quarks are related to the formation of these states and the quark flavor content can be specified through Cabibbo-favored and -suppressed processes [16]. Additionally, the dynamics of the SL charmed meson decays can be studied by measuring the hadronic form factor (FF) that describes the strong interaction between the final-state quarks, including all the non-perturbative effects. This provides an excellent opportunity to test the different theoretical methods of solving the QCD non-perturbative problem. Since the FFs and branching fractions (BFs) of the SL charmed meson decays are highly sensitive to the internal structure of light scalar states, studies of the dynamics of these decays are also important to understand their nature [12].

In previous studies, the BESIII collaboration has reported measurements of the decays $D^{0(+)} \rightarrow a_0(980)^{-(0)} e^+ \nu_e$ [17], $D^+ \rightarrow f_0(500) e^+ \nu_e$ [18], and $D_s^+ \rightarrow f_0(980) e^+ \nu_e, f_0(980) \rightarrow \pi^0 \pi^0$ [19], and searches for the decays $D^+ \rightarrow f_0(980) e^+ \nu_e$ and $D_s^+ \rightarrow a_0(980)^0 e^+ \nu_e$ [18, 20]. With negligible contamination from the $D_s^+ \rightarrow \rho^0 e^+ \nu_e$ channel, the decay $D_s^+ \rightarrow \pi^+ \pi^- e^+ \nu_e$ enables us to study the structure of $f_0(980)$ in a clean environment. Previously, only the CLEO collaboration measured the BF of the decay $D_s^+ \rightarrow f_0(980) e^+ \nu_e, f_0(980) \rightarrow \pi^+ \pi^-$ [21–23] with data taken at a center-of-mass (CM) energy (E_{CM}) near 4.170 GeV. With a data sample more than 10 times larger, we report a significantly improved measurement of the BF and the first measurement of the transition FF. The obtained results are important tests of theoretical predictions based on different models [6–12]. Throughout this letter, charge-conjugate channels are implied.

For the BF measurements of SL decays, we use the same double-tag technique of Refs [19, 20, 24]. Our measurements are performed based on $e^+ e^-$ collision data corresponding to an integrated luminosity of 7.33 fb^{-1} collected with the BESIII detector at $E_{\text{CM}} = 4.128 - 4.226 \text{ GeV}$ [25]. Details about the BESIII detector design and performance are provided in Refs. [26–28].

Simulated data samples produced with a GEANT4-based [30] Monte Carlo (MC) package, which includes the geometric description of the BESIII detector [29] and the detector response, are used to determine detection efficiencies and to estimate backgrounds. The simulation models the beam energy spread and initial state radiation (ISR) in the $e^+ e^-$ annihilations with the generator KKMC [31]. The inclusive MC sample includes the production of open-charm processes, the ISR production of vector charmonium(-like) states, and the continuum pro-

cesses incorporated in KKMC [31]. All particle decays are modelled with EVTGEN [32] using BFs either taken from the Particle Data Group [4], when available, or otherwise estimated with LUNDCHARM [33]. Final state radiation from charged final state particles is incorporated using the PHOTOS package [34]. The signal detection efficiencies and signal shapes are obtained from the signal MC samples, in which the D_s^- decays inclusively to all known decay channels and the signal D_s^+ decays to $\pi^+ \pi^- e^+ \nu_e$ with the S -wave contribution simulated according to previous measurements [18, 35]. The amplitudes for the $f_0(980)$ is modeled by the Flatté formula with its parameters fixed to the BESII measurement [36].

The tag D_s^- candidates are reconstructed with $K^\pm, \pi^\pm, \rho^0, \rho^0, \eta^0, \eta^{'},$ and K_S^0 mesons in twelve tag modes: $K^+ K^- \pi^-$, $K_S^0 K^-$, $\pi^- \eta$, $\pi^- \eta'_{\pi^+ \pi^- \eta}$, $K^+ K^- \pi^- \pi^0$, $\pi^+ \pi^- \pi^-$, $K_S^0 K^+ \pi^- \pi^-$, $\rho^- \eta$, $\pi^- \eta'_{\rho^0}$, $K^+ \pi^- \pi^-$, $K_S^0 K^- \pi^0$, and $K_S^0 K^- \pi^+ \pi^-$. A detailed description of the selection criteria for all tag candidates except $\rho^- \eta$ can be found in Ref [37]. The ρ^- candidates are reconstructed from $\pi^- \pi^0$ combinations within an invariant mass interval $(0.625, 0.925) \text{ GeV}/c^2$. Requirements on the recoiling mass m_{rec} against the tag D_s^- candidates are applied to the tag candidates in order to identify the process $e^+ e^- \rightarrow D_s^{*\pm} D_s^\mp$. If there are multiple candidates for a specific tag mode per charge, the one with m_{rec} closest to the known $D_s^{*\pm}$ mass [4] is chosen. For each tag mode, the tag yield is extracted from the fit to the tag D_s^- mass spectrum ($M_{D_s^-}$). The signals are modeled with the MC-simulated signal shape convolved with a Gaussian function to account for the resolution difference between data and MC simulation, while the combinatorial backgrounds are parameterized with a first-order or second-order Chebyshev polynomial. For the tag mode $D_s^- \rightarrow K_S^0 K^-$, the peaking background from $D^- \rightarrow K_S^0 \pi^-$ decay is described by the MC-simulated shape that is smeared with the same Gaussian function as used in the signal, with the background yield determined from the fit. Summing over various tag modes and energy points, we obtain the total tag yield $N_{\text{tag}}^{\text{tot}} = 771101 \pm 3445$. For more details about tag candidates, such as selection regions and reconstruction efficiencies, see Ref. [25].

After a D_s^- candidate is identified, we reconstruct the decay $D_s^+ \rightarrow \pi^+ \pi^- e^+ \nu_e$ recoiling against the tag side, requiring three charged tracks identified as a $\pi^+ \pi^-$ pair with the same selection criteria as on the tag side and e^+ (opposite sign to the tag D_s^-) following Ref. [38]. Using the same kinematic fit method of Refs [19, 20, 24], we reconstruct the transition photon from the main decay $D_s^{*\pm} \rightarrow \gamma D_s^\pm$.

For the real $D_s^{*\pm} D_s^\mp$ events, the square of the recoil mass (M_{rec}^2) against the transition photon and the tag D_s^- is expected to peak at the known D_s^+ mass squared. To improve the resolution, the decay products of the tag

D_s^- are constrained to the known D_s^+ mass [4]. We require M_{rec}^2 to be within $(3.78, 4.05) \text{ GeV}^2/c^4$ to suppress the backgrounds from non- $D_s^{*\pm}D_s^\mp$ processes. The missing neutrino information is inferred by the missing mass squared which is defined as

$$M_{\text{miss}}^2 = (\mathbf{p}_{\text{CM}} - \mathbf{p}_{\text{tag}} - \mathbf{p}_{\pi^+} - \mathbf{p}_{\pi^-} - \mathbf{p}_e - \mathbf{p}_\gamma)^2, \quad (1)$$

where \mathbf{p}_{CM} is the four-momentum of the e^+e^- center-of-mass system, \mathbf{p}_{tag} for the tag D_s^- , $\mathbf{p}_{\pi^+(\pi^-, e)}$ for the SL final state, and \mathbf{p}_γ for the transition photon from the $D_s^{*\pm}$ decay. Here, the measured momenta of the tag D_s^- and the transition photon are corrected with the kinematic fit to improve the resolution. In order to further reject backgrounds, we require $|M_{\text{miss}}^2| < 0.06 \text{ GeV}^2/c^4$.

To study the $f_0(980)$, we require the $\pi^+\pi^-$ invariant mass ($M_{\pi^+\pi^-}$, see Fig. 1) to be within the interval $(0.6, 1.6) \text{ GeV}/c^2$. The weighted signal efficiency is $(35.44 \pm 0.07)\%$, which is estimated as $\sum_i [(N_{\text{tag}}^i/N_{\text{tag}}^{\text{tot}}) \times (\epsilon_{\text{tag}}^i/\epsilon_{\text{tag,sig}}^i)]$, where $N_{\text{tag}}^{\text{tot}}$ is the total tag yield, and ϵ_{tag}^i and $\epsilon_{\text{tag,sig}}^i$ are the tag and SL efficiencies for the i -th tag mode, respectively. The non-peaking background distribution from the inclusive MC sample is verified using events from the data sideband region (about 2σ away from the signal region of the tag D_s^- mass and having the same interval as signal region) of the tag $M_{D_s^-}$ distribution. The peak around $0.75 \text{ GeV}/c^2$ is mainly caused by the decay $D_s^+ \rightarrow \eta'(\gamma\pi^+\pi^-)e^+\nu_e$. An unbinned maximum likelihood fit to the $M_{\pi^+\pi^-}$ distribution is performed to extract the SL signal yield of $D_s^+ \rightarrow f_0(980)e^+\nu_e$, $f_0(980) \rightarrow \pi^+\pi^-$ decay. In the fit, the signal is modeled with an MC-simulated lineshape convolved with a Gaussian resolution function, and the background is described by the inclusive MC shape convolved with the same Gaussian function as the signal. From the fit, which is shown in Fig. 1, we obtain 439 ± 33 signal events. Using the tag and SL efficiencies provided in Ref. [25], we obtain $\mathcal{B}(D_s^+ \rightarrow f_0(980)e^+\nu_e, f_0(980) \rightarrow \pi^+\pi^-) = (1.72 \pm 0.13_{\text{stat}} \pm 0.10_{\text{syst}}) \times 10^{-3}$, where the uncertainties are statistical and systematic, respectively.

The systematic uncertainties of the tracking or particle identification (PID) efficiencies of π^\pm and e^\pm are studied with control samples of $e^+e^- \rightarrow K^+K^-\pi^+\pi^-$ and $e^+e^- \rightarrow \gamma e^+e^-$ processes. For e^+ both the tracking and PID uncertainties are assigned to be 0.5%. For π^\pm both uncertainties are also assigned to be 0.5% per track, or 1.0% for the $\pi^+\pi^-$ pair. The uncertainty from the quoted BF of $D_s^{*\pm} \rightarrow \gamma D_s^\pm$ decay is 0.7% [4]. The uncertainty due to the transition photon reconstruction is estimated to be 2.0% using the control sample of $e^+e^- \rightarrow D_s^{*\pm}D_s^\mp$ events, where D_s^- decays via a tag mode, while D_s^+ decays via one of the two hadronic channels: $D_s^+ \rightarrow K_S^0 K^+$ or $D_s^+ \rightarrow K^+ K^- \pi^+$. The uncertainty in the total number of the tag D_s^- mesons is assigned to be 0.3% by examining the changes of the fit yields when varying the signal shape, background shape, and taking into account

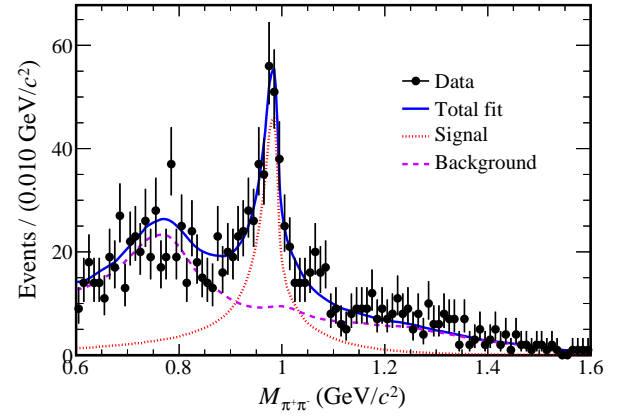


FIG. 1. Fit to the $M_{\pi^+\pi^-}$ distribution of the accepted candidates for the decay $D_s^+ \rightarrow f_0(980)e^+\nu_e$. The points with error bars are data, and the blue line is the total fit. The red dotted and violet dashed lines are the signal and background shapes, respectively.

the background fluctuation in the fit. The uncertainty associated with the signal MC model is estimated to be 4.4% by replacing the $f_0(980)$ lineshape from BESII [36] with the one from LHCb [39] in generating the signal MC samples. The uncertainties of the $M_{\pi^+\pi^-}$ fit is estimated to be 2.1% by altering the nominal MC background shape. Firstly, we use alternative MC shapes where the relative fractions of backgrounds from continuum and non- $D_s^{*\pm}D_s^\mp$ open-charm processes are varied by $\pm 30\%$ according to the uncertainties of their assigned cross sections in the inclusive MC sample. Secondly, we vary the relative fraction ($\pm 1\sigma$) of the peaking background channel $D_s^+ \rightarrow \eta'(\gamma\pi^+\pi^-)e^+\nu_e$ [4]. The total systematic uncertainty is 5.6%, obtained by adding all contributions in quadrature.

The dynamics of $D_s^+ \rightarrow f_0(980)e^+\nu_e$ decay is studied by dividing the SL candidate events into four intervals of q^2 (four-momentum transfer square of $e^+\nu_e$). Using the measured and expected partial decay rates of the i -th q^2 interval, $\Delta\Gamma_{\text{mea}}^i$ and $\Delta\Gamma_{\text{exp}}^i$, the FF is determined by constructing and minimizing a χ^2 as

$$\chi^2 = \sum_{ij} (\Delta\Gamma_{\text{mea}}^i - \Delta\Gamma_{\text{exp}}^i) C_{ij}^{-1} (\Delta\Gamma_{\text{mea}}^j - \Delta\Gamma_{\text{exp}}^j), \quad (2)$$

where C_{ij} is the covariance matrix to consider correlations of $\Delta\Gamma_{\text{mea}}^i$ among q^2 intervals.

The $\Delta\Gamma_{\text{exp}}^i$ is calculated by integrating the following double differential decay rate [40]

$$\begin{aligned} \frac{d^2\Gamma(D_s^+ \rightarrow f_0(980)e^+\nu_e)}{dsdq^2} &= \frac{G_F^2 |V_{cs}|^2}{192\pi^4 m_{D_s^+}^3} \lambda^{3/2} (m_{D_s^+}^2, s, q^2) \\ &\times |f_+^{f_0}(q^2)|^2 P(s), \end{aligned} \quad (3)$$

where s is the square of $M_{\pi^+\pi^-}$, G_F is the Fermi constant [4], $|V_{cs}|$ is the Cabibbo Kobayashi-Maskawa matrix element, $m_{D_s^+}$ is the known D_s^+ mass [4], $\lambda(x, y, z) = x^2 + y^2 + z^2 - 2xy - 2xz - 2yz$, and $P(s)$ is based on the relativistic Flatté formula [36] due to the open K^+K^- channel in data as follows:

$$P(s) = \frac{g_1 \rho_{\pi\pi}}{|m_0^2 - s - i(g_1 \rho_{\pi\pi} + g_2 \rho_{K\bar{K}})|^2}. \quad (4)$$

Here m_0 denotes the $f_0(980)$ mass; the constants g_1 and g_2 are the $f_0(980)$ couplings to $\pi^+\pi^-$ and K^+K^- final states, respectively; and $\rho_{\pi\pi}$ and $\rho_{K\bar{K}}$ are individual phase space factors. Using the decay widths in the different q^2 intervals, the FF $|f_+^{f_0}(q^2)|$ can be extracted. In this work, the FF is modeled with the simple pole parameterization [44]:

$$f_+^{f_0}(q^2) = \frac{f_+^{f_0}(0)}{1 - q^2/M_{\text{pole}}^2}, \quad (5)$$

where $f_+^{f_0}(0)$ is the FF evaluated at $q^2 = 0$, and the pole mass $M_{\text{pole}} = 2.46 \text{ GeV}/c^2$ [4, 41].

The measured partial decay rate $\Delta\Gamma_{\text{mea}}^i$ is determined by $\Delta\Gamma_{\text{mea}}^i \equiv \int_s \int_s \frac{d^2\Gamma}{dsdq^2} dsdq^2 = N_{\text{pro}}^i / (\tau N_{\text{tag}}^{\text{tot}} \mathcal{B}_\gamma)$, where \mathcal{B}_γ represents the BF of $D_s^{*\pm} \rightarrow \gamma D_s^\pm$, τ is the D_s^+ meson lifetime [4, 42] and N_{pro}^i is the SL signal yield produced in the i -th q^2 interval, obtained as $N_{\text{pro}}^i = \sum_{j=1}^4 \epsilon_{ij}^{-1} N_{\text{obs}}^j$. Here N_{obs}^j is the observed SL decay yield obtained from the similar fit to the corresponding $M_{\pi^+\pi^-}$ distribution as described previously, and ϵ_{ij} is the efficiency matrix determined from the signal MC samples via $\epsilon_{ij} = \sum_k [(1/N_{\text{tag}}^{\text{tot}}) \times (N_{\text{rec}}^{ij}/N_{\text{gen}}^j) \times (N_{\text{tag}}^k/\epsilon_{\text{tag}}^k)]$, where N_{rec}^{ij} is the SL decay yield reconstructed in the i -th q^2 interval and generated in the j -th q^2 interval, N_{gen}^j is the total signal yield generated in the j -th q^2 interval, and k sums over all tag modes. The details of the divisions, N_{obs}^j and $\Delta\Gamma_{\text{mea}}^i$ of various q^2 intervals are given in Ref. [25].

The statistical and systematic covariance matrices are constructed as $C_{ij}^{\text{stat}} = (1/\tau N_{\text{tag}}^{\text{tot}})^2 \sum_\alpha \epsilon_{i\alpha}^{-1} \epsilon_{j\alpha}^{-1} [\sigma(N_{\text{obs}}^\alpha)]^2$ and $C_{ij}^{\text{syst}} = \delta(\Delta\Gamma_{\text{mea}}^i) \delta(\Delta\Gamma_{\text{mea}}^j)$, respectively, where $\sigma(N_{\text{obs}}^\alpha)$ and $\delta(\Delta\Gamma_{\text{mea}}^i)$ are the statistical and systematic uncertainties in the i -th q^2 interval. The C_{ij}^{syst} is obtained by summing all the covariance matrices for all systematic uncertainties, where the systematic uncertainty of τ , 0.8% [4, 42], is involved besides those in the BF measurement. The obtained C_{ij}^{stat} and C_{ij}^{syst} are shown in Ref. [25]. The resulting C_{ij} is obtained as $C_{ij} = C_{ij}^{\text{stat}} + C_{ij}^{\text{syst}}$.

The statistical and systematic uncertainties related to C_{ij} and $\Delta\Gamma_{\text{mea}}^i$ are estimated to be 3.4% and 2.6% by following Ref [43]. Besides, the input parameters m_0 , g_1 , and g_2 [36] related to $\Delta\Gamma_{\text{exp}}^i$ are also considered by varying them within $\pm 1\sigma$ from their central values. The largest deviations of the FF, respectively 2.2%, 1.2% and

6.0%, are taken as systematic uncertainties. The quadrature sum of the above uncertainties is 6.9%, which is taken as the total systematic uncertainty.

The fit to the differential decay rate of the channel $D_s^+ \rightarrow f_0(980)e^+\nu_e$ and the FF projection are shown in Fig. 2. Using the FF parameterization of Eq. 3 and the Flatté formula Eq. 4 for the $f_0(980)$ decay in the fit, the product of the FF and $|V_{cs}|$ is determined to be $f_+^{f_0}(0)|V_{cs}| = 0.504 \pm 0.017_{\text{stat}} \pm 0.035_{\text{syst}}$. The fit result is shown in Fig. 2 (a), while Fig. 2 (b) shows the same fit in projection to the FF $f_+^{f_0}(q^2)$. The goodness of fit χ^2/NDF is 0.8, where NDF is the number of degrees of freedom.

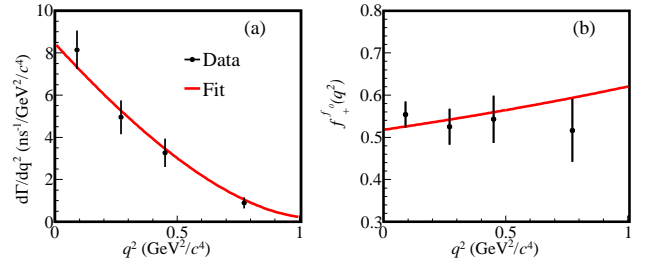


FIG. 2. Fit to the differential decay rate as a function of q^2 (a) and projection to the FF $f_+^{f_0}(q^2)$ (b). The points with error bars are data, and the red line is the fit.

In summary, using e^+e^- collision data corresponding to an integrated luminosity of 7.33 fb^{-1} collected at $E_{\text{CM}} = 4.128 - 4.226 \text{ GeV}$ by the BESIII detector, we measure the BF of $D_s^+ \rightarrow f_0(980)e^+\nu_e$, $f_0(980) \rightarrow \pi^+\pi^-$ decay to be $(1.72 \pm 0.13_{\text{stat}} \pm 0.10_{\text{syst}}) \times 10^{-3}$, which is 2.6 times more accurate than the previous measurement [23]. Using the relation between the BF and the mixing angle ϕ involved in the $q\bar{q}$ mixture picture for $f_0(980)$ as $\sin\phi \frac{1}{\sqrt{2}}(u\bar{u} + d\bar{d}) + \cos\phi s\bar{s}$ [8, 11], we find that the $s\bar{s}$ component is dominant. This conclusion disagrees with that in Ref. [11] where their calculation is based on the CLEO measurement [21].

Furthermore, we determine $f_+^{f_0}(0)|V_{cs}| = 0.504 \pm 0.017_{\text{stat}} \pm 0.035_{\text{syst}}$ for the first time by analyzing the dynamics of $D_s^+ \rightarrow f_0(980)e^+\nu_e$, $f_0(980) \rightarrow \pi^+\pi^-$ decay. Using $|V_{cs}| = 0.97349 \pm 0.00016$ [4], we obtain $f_+^{f_0}(0) = 0.518 \pm 0.018_{\text{stat}} \pm 0.036_{\text{syst}}$. In Table I the measured FF result at $q^2 = 0$ is compared with different theoretical predictions. Our measurement agrees with the theoretical results in Refs. [6–8], but is much higher than the theoretical results in Refs. [9, 11, 12]. It is notable that most predicted FF $f_+^{f_0}(0)$ and BF depend on the angle ϕ known with large uncertainty. So, the measured FF and BF are both important to constrain this angle and probe the quark component in $f_0(980)$ [11]. Although most theoretical predictions for $f_+^{f_0}(0)$ have a large uncertainty due to the ϕ uncertainty, the measured

FF lineshape is a powerful tool to distinguish different models. These results are important to understand the nature of the light scalar states $f_0(980)$ and the non-perturbative dynamics of charm meson decays.

The BESIII Collaboration thanks the staff of BEPCII and the IHEP computing center for their strong support. The authors are grateful to De-Liang Yao, Shan Cheng and Xian-Wei Kang for valuable discussions. This work is supported in part by National Key R&D Program of China under Contracts Nos. 2020YFA0406300, 2020YFA0406400; National Natural Science Foundation of China (NSFC) under Contracts Nos. 11635010, 11735014, 11835012, 11935015, 11935016, 11935018, 11961141012, 12022510, 12025502, 12035009, 12035013, 12061131003, 12192260, 12192261, 12192262, 12192263, 12192264, 12192265; Natural Science Foundation of Hunan Province, China under Contract No. 2021JJ40036 and the Fundamental Research Funds for the Central Universities under Contract No. 020400/531118010467; the Chinese Academy of Sciences (CAS) Large-Scale Scientific Facility Program; the CAS Center for Excellence in Particle Physics (CCEPP); Joint Large-Scale Scientific Facility Funds of the NSFC and CAS under Contract No. U1832207; CAS Key Research Program of

Frontier Sciences under Contracts Nos. QYZDJ-SSW-SLH003, QYZDJ-SSW-SLH040; 100 Talents Program of CAS; The Institute of Nuclear and Particle Physics (IN-PAC) and Shanghai Key Laboratory for Particle Physics and Cosmology; ERC under Contract No. 758462; European Union's Horizon 2020 research and innovation programme under Marie Skłodowska-Curie grant agreement under Contract No. 894790; German Research Foundation DFG under Contracts Nos. 443159800, 455635585, Collaborative Research Center CRC 1044, FOR5327, GRK 2149; Istituto Nazionale di Fisica Nucleare, Italy; Ministry of Development of Turkey under Contract No. DPT2006K-120470; National Research Foundation of Korea under Contract No. NRF-2022R1A2C1092335; National Science and Technology fund of Mongolia; National Science Research and Innovation Fund (NSRF) via the Program Management Unit for Human Resources & Institutional Development, Research and Innovation of Thailand under Contract No. B16F640076; Polish National Science Centre under Contract No. 2019/35/O/ST2/02907; The Royal Society, UK under Contract No. DH160214; The Swedish Research Council; U. S. Department of Energy under Contract No. DE-FG02-05ER41374.

TABLE I. Comparison of the FF at $q^2 = 0$ between our measurement and various theoretical predictions.

	This work	CLFD [6]	DR [6]	QCDSR [7]	QCDSR [8]	LCSR [9]	LFQM [11]	CCQM [12]
$f_+^{J_0}(0)$	$0.518 \pm 0.018_{\text{stat}} \pm 0.036_{\text{syst}}$	0.45	0.46	0.50 ± 0.13	0.48 ± 0.23	0.30 ± 0.03	0.24 ± 0.05	0.39 ± 0.02
Difference (σ)	—	—	—	0.1	0.2	4.3	4.3	2.8
ϕ in theory	—	$(32 \pm 4.8)^\circ$	$(41.3 \pm 5.5)^\circ$	35°	$(8_{-8}^{+21})^\circ$	—	$(56 \pm 7)^\circ$	31°

-
- [1] J. R. Peláez, Phys. Rept. **658**, 1 (2016).
 - [2] W. Wang and C. D. Lu, Phys. Rev. D **82**, 034016 (2010).
 - [3] R. L. Jaffe, Phys. Rev. D **15**, 267 (1977).
 - [4] R. L. Workman *et al.* (Particle Data Group), Prog. Theor. Exp. Phys. **2022**, 083C01 (2022).
 - [5] V. V. Anisovich, L. Montanet, and V. N. Nikonov, Phys. Lett. B **480**, 19-22 (2000).
 - [6] B. El-Bennich, O. Leitner, J. P. Dedonder, and B. Loiseau, Phys. Rev. D **79**, 076004 (2009).
 - [7] I. Bediaga, F. S. Navarra, and M. Nielsen, Phys. Lett. B **579**, 59-66 (2004).
 - [8] T. M. Aliev and M. Savci, EPL **90**, 61001 (2010).
 - [9] P. Colangelo, F. D. Fazio, and W. Wang, Phys. Rev. D **81**, 074001 (2010).
 - [10] Y. J. Shi and W. Wang, Phys. Rev. D **92**, 074038 (2015).
 - [11] H. W. Ke, X. Q. Li, and Z. T. Wei, Phys. Rev. D **80**, 074030 (2009).
 - [12] N. R. Soni, A. N. Gadaria, J. J. Patel, and J. N. Pandya, Phys. Rev. D **102**, 016013 (2020).
 - [13] J. R. Peláez, Phys. Rev. Lett. **92**, 102001 (2004); N. N. Achasov and A. V. Kiselev, Phys. Rev. D **73**, 054029 (2006); G. 't Hooft, G. Isidori, L. Maiani, A. D. Polosa, and V. Riquer, Phys. Lett. B **662**, 424 (2008); A. H. Fariborz, R. Jora,

- and J. Schechter, Phys. Rev. D **79**, 074014 (2009); S. Weinberg, Phys. Rev. Lett. **110**, 261601 (2013); H. C. Kim, K. S. Kim, M. K. Cheoun, Daisuke Jido, and Makoto Oka, Phys. Rev. D **99**, 014005 (2019).
- [14] J. Weinstein and N. Isgur, Phys. Rev. D **41**, 2236 (1990); T. Branz, T. Gutsche, and V. Lyubovitskij, Eur. Phys. J. A **37**, 303–317 (2008); L. Y. Dai, X. G. Wang, and H. Q. Zheng, Commun. Theor. Phys. **58**, 410 (2012); L. Y. Dai and M. R. Pennington Phys. Lett. B **736**, 11-15 (2014); T. Sekihara and S. Kumano, Phys. Rev. D **92**, 034010 (2015); D. L. Yao, L. Y. Dai, H. Q. Zheng, and Z. Y. Zhou, Rep. Prog. Phys. **84**, 076201 (2021); Z. Q. Wang, X. W. Kang, J. A. Oller, and L. Zhang, Phys. Rev. D **105**, 074016 (2022).
- [15] N. N. Achasov and A. V. Kiselev, Phys. Rev. D **86**, 114010 (2012).
- [16] T. Sekihara and E. Oset, Phys. Rev. D **92**, 054038 (2015).
- [17] M. Ablikim *et al.* (BESIII Collaboration), Phys. Rev. Lett. **121**, 081802 (2018).
- [18] M. Ablikim *et al.* (BESIII Collaboration), Phys. Rev. Lett. **122**, 062001 (2019).
- [19] M. Ablikim *et al.* (BESIII Collaboration), Phys. Rev. D **105**, L031101 (2022).

- [20] M. Ablikim *et al.* (BESIII Collaboration), Phys. Rev. D **103**, 092004 (2021).
- [21] J. Yelton *et al.* (CLEO Collaboration), Phys. Rev. D **80**, 052007 (2009).
- [22] K. M. Ecklund *et al.* (CLEO Collaboration), Phys. Rev. D **80**, 052009 (2009).
- [23] J. Hietala, D. Cronin-Hennessy, T. Pedlar, and I. Shipsey, Phys. Rev. D **92**, 012009 (2015).
- [24] M. Ablikim *et al.* (BESIII Collaboration), Phys. Rev. D **99**, 031101(R) (2019).
- [25] See Supplemental Material at [URL] for additional analysis information.
- [26] M. Ablikim *et al.* (BESIII Collaboration), Nucl. Instrum. Methods Phys. Res., Sect. A **614**, 345 (2010).
- [27] M. Ablikim *et al.* (BESIII Collaboration), Chin. Phys. C **44**, 040001 (2020).
- [28] X. Li *et al.*, Radiat. Detect. Technol. Methods 1, 13 (2017); Y. X. Guo *et al.*, Radiat. Detect. Technol. Methods 1, 15 (2017).
- [29] K. X. Huang *et al.*, Nucl. Sci. Tech. **33**, 142 (2022).
- [30] S. Agostinelli *et al.* (GEANT4 Collaboration), Nucl. Instrum. Meth. A **506**, 250 (2003).
- [31] S. Jadach, B. F. L. Ward and Z. Was, Comput. Phys. Commun. **130**, 260 (2000); Phys. Rev. D **63**, 113009 (2001).
- [32] D. J. Lange, Nucl. Instrum. Meth. A **462**, 152 (2001); R. G. Ping, Chin. Phys. C **32**, 599 (2008).
- [33] J. C. Chen, G. S. Huang, X. R. Qi, D. H. Zhang and Y. S. Zhu, Phys. Rev. D **62**, 034003 (2000); R. L. Yang, R. G. Ping and H. Chen, Chin. Phys. Lett. **31**, 061301 (2014).
- [34] E. Richter-Was, Phys. Lett. B **303**, 163 (1993).
- [35] M. Ablikim *et al.* (BESIII Collaboration), Phys. Rev. D **94**, 032001 (2016).
- [36] M. Ablikim *et al.* (BES Collaboration), Phys. Lett. B **607**, 243 (2005).
- [37] M. Ablikim *et al.* (BESIII Collaboration), J. High Energ. Phys. **04**, 058 (2022).
- [38] M. Ablikim *et al.* (BESIII Collaboration), Phys. Rev. D **92**, 071101(R) (2015).
- [39] R. Aaij *et al.* (LHCb Collaboration), Phys. Rev. D **86**, 052006 (2012).
- [40] W. Wang, Phys. Rev. B **759**, 501 (2016). The form of our double differential decay rate is a little different but consistent with this reference by redefining the parameters of Flatté formula.
- [41] N. N. Achasov, A. V. Kiselev, and G. N. Shestakov, Phys. Rev. D **102**, 016022 (2020).
- [42] R. Aaij *et al.* (LHCb Collaboration), Phys. Rev. Lett. **119**, 101801 (2017).
- [43] M. Ablikim *et al.* (BESIII Collaboration), Phys. Rev. D **92**, 072012 (2015).
- [44] D. Becirevic and A. B. Kaidalov, Phys. Lett. B **478**, 417 (2000).